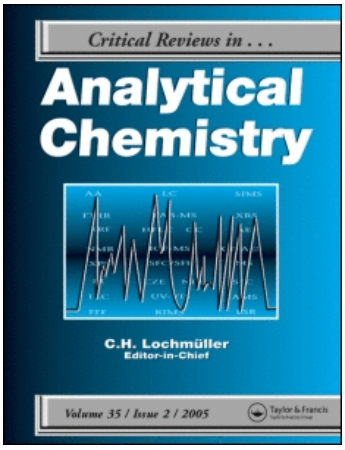

Critical Reviews in Analytical Chemistry
Publication details, including instructions for authors and subscription information:
http://www.informaworld.com/smpp/title~content=t713400837

Depth Profiling in Thin Dielectric Films

P. W. Bohn[a]; D. R. Miller[b]
[a] Departments of Chemistry and Beckman Institute, University of Illinois at Urbana-Champaign, Urbana, IL [b] Dow Chemical Corp., Midland, MI

To cite this Article Bohn, P. W. and Miller, D. R.(1991) 'Depth Profiling in Thin Dielectric Films', Critical Reviews in Analytical Chemistry, 22: 1, 455 — 470
To link to this Article: DOI: 10.1080/10408349108055023
URL: http://dx.doi.org/10.1080/10408349108055023

Critical Reviews in Analytical Chemistry, 22(1,2):455—470 (1991)

Depth Profiling in Thin Dielectric Films

P. W. Bohn

Department of Chemistry and Beckman Institute, University of Illinois at Urbana-Champaign, 1209 W. California St., Urbana, IL 61801

D. R. Miller

Dow Chemical Corp., 1897 Bldg., Midland, MI 48667

ABSTRACT: Thin polymer films occupy an eminent position in modern science and technology both in and of themselves and as models for bulk polymer systems. Much of their function depends on their interaction with external (often hostile) environments. Thus, methods for obtaining information about the chemistry of these films as a function of depth are a critical need. This review critically evaluates the methods which have been applied up to this point for depth profiling in polymers and concentrates on two methods: optical depth profiling using excitation in a slab waveguide, and nuclear reaction profiling. Guided wave experiments have been useful in situations in which the species being determined forms only a minor or trace constitutent of the thin film matrix, while nuclear reaction profiling has been applied primarily to profiles of protonated and deuterated polymers in studies of interdiffusion. Other techniques for depth profiling have more limited applications.

KEY WORDS: thin film, Raman scattering, inversion techniques, spectroscopy.

I. INTRODUCTION

Thin organic films are an important aspect of modern research and technology, being employed for applications including optical coatings,[1-9] integrated optics,[8,10-17] semi-permeable membranes,[18,19] electrocatalysis at surface modified electrodes,[20-23] solar energy conversion schemes,[24-28] and protective coatings.[29-31] Optimal design and use of thin organic films require a thorough understanding of the system chemistry and structure. While information about film thickness and refractive indices in most cases can be achieved by one of several methods (including ellipsometry, reflectometry, and measurement of the eigenmode distribution of an optical waveguide[8,15,32-49] and mapping in the lateral direction can be performed via several well-established techniques, applicable techniques for depth profiling of composition in thin dielectric films are limited. Depth profiling is desirable for comprehensive studies of structure-function relations, diffusion, and reactive-site behavior in thin films. Furthermore, an understanding of the compositional depth profile in a thin film sample is essential because the bulk of a film is frequently dissimilar from the interfacial regions in both composition and structure.

As an example of a situation in which depth profiling would be highly valuable, consider studies of antenna molecules for energy concentration at solar energy conversion centers. The energy transport efficiency is extremely sensitive to the distance between the antenna and the reaction center.[28] Since the number densities of the reaction centers and antenna molecules may vary as a function of depth (e.g., due to phase separation during sample fabrication), the distribution of separation distances between the antenna and reaction center may also be depth dependent, which would lead to a depth-dependent behavior of the thin film system. Knowing the number

1040-8347/91/$.50

densities of donors, acceptors, and traps in each spatial region would allow a more exact comparison between energy transfer efficiency and separation distances. Such studies should also help clarify which energy transport mechanisms are most important in a particular system.

Several depth profiling techniques have been developed, each having different, and frequently limited, capabilities. In this paper, we discuss each of the depth profiling techniques which have been developed, with a critical eye toward the strengths and weaknesses of each and the situations in which they may appropriately be applied.

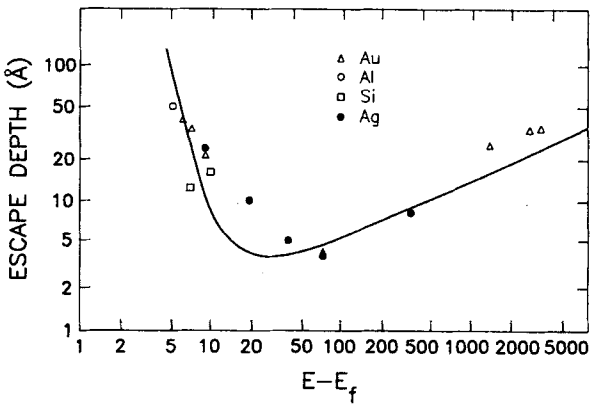

FIGURE 1. Plot of the mean electron escape depth, i.e., the mean depth from which an electron can escape without suffering an inelastic collision, as a function of electron energy for Si, Al, Ag, and Au. Data were compiled from various literature sources.

II. HIGH VACUUM TECHNIQUES FOR DEPTH PROFILING IN DIELECTRIC FILMS

Several depth profiling methods have been developed which rely upon high vacuum spectroscopic techniques. For example, since the electron escape depth for elastic electrons generated from photoionization events is so small (typically <100 Å), the angular distribution of electrons obtained in an X-ray photoelectron spectroscopy (XPS) experiment carries information about the spatial distribution of composition. Angular distribution XPS has shown some success for depth profiling in dielectric films of 100 Å thickness or less.[50-54] Unfortunately, in order to extract highly accurate depth maps of composition, it is necessary to have a very accurate description of the probability that an electron will escape, if it starts from a particular depth. Because the electron escape depths cannot be independently determined, estimates must be made which cause large positional uncertainties (ca. ± 50%). As shown in Figure 1, this probability is matrix and electron energy dependent, and so it is almost never known with quantitative accuracy. In addition, at a given angle, electrons contribute to the signal from a distribution of depths from within the sample, and the form of this distribution is typically not well known. Thus, inadequate knowledge of electron escape depths of the sampled films represents a major limitation in this technique. Of course, this experiment would not be appropriate to the study of buried interfaces without the inclusion of some type of sputtering to remove the overlying material. There are very serious challenges in performing any type of sputtering experiment and obtaining quantitative accuracy *(vide infra)*. Other sources of error include nonlinear effects which result from surface irregularities. On the other hand, the inherent resolution is quite high (of the order of a few angstroms) because the electron escape probability is a sharp function of depth, and chemical speciation information can be obtained due to site-specific binding energy shifts. If information is desired with the ultimate spatial resolution, it is perhaps the only choice.

Angle lapping and cross-sectioning techniques followed by scanning surface detection methods are feasible depth profiling techniques for samples with sufficient rigidity.[8,55-57] Typically, a beveled (1 to 5°) sample block is fabricated, and the sample is subjected to mechanical abrasion to remove material along an angular profile. Then, a convenient compositional probe with high lateral resolution (i.e., small excitation spot size) can be used to convert depth information into lateral information. Of course, the shallower the angle, the greater the depth resolution which can be achieved. With 0.5° angle lap, a 1.0-μm spot size would correspond to 90 Å depth resolution. Unfortunately, organic polymer films generally lack adequate rigidity to ensure the preservation of the profile during the physical angle lapping process, and mechanical abrasion

always has the potential to introduce impurities into the sample. Thus, angle lapping tends to be more highly favored among mechanically harder materials. These will include many materials of interest for their electronic and optical properties.

Secondary ion mass spectroscopy (SIMS) is a well-known technique which has been very successfully employed for depth profiling in conductive materials, displaying a typical resolution of 2.5 Å.[58,59] When applied to nonconductors, however, the situation is more difficult. Quantitative accuracy is very difficult to obtain due to the notorious matrix effects which attend SIMS signals. The applicability of SIMS is further limited because the attainable resolution and dynamic range are frequently restricted by uneven sputtering rates, cascade mixing, and redeposition effects. Of these three problems, redeposition effects can be eliminated by cross-sectioning the sample via sputtering at shallow incident angles to create a beveled region.[60] The region can then be laterally profiled using scanning Auger spectroscopy or an ion microprobe,[61,62] and the lateral profile is directly related to the depth profile via the angle of sectioning. However, resolution is still limited by uneven sputtering rates and cascade mixing.

Unfortunately, beam damage and extensive charging present major difficulties for depth profiling nonconductive materials via sputtering. Following the lead of investigators working on electron spectroscopy of nonconductive materials, some success has been obtained in profiling Na^+ in SiO_2 by neutralizing the material with a carefully controlled electron beam dosage.[63] Despite the author's suggestions of simplicity, however, the technique has not been frequently utilized.[59] Depth profiling in organic polymer matrices is even more difficult due to substantial polymer degradation which leads to highly variable sputtering rates[59,64,65] and to changes in chemical speciation. Nonetheless, Linton and coworkers have recently profiled a Ru complex doped into a 1-μm thick chlorosulfonated polystyrene film using SIMS.[66] The approach attempted to account for variable sampling rates by using an internal standard. Although their results were dramatically improved compared to uncompensated samples, other sampling difficulties, including momentum transfer and redeposition effects, were not reliably compensated, resulting in a low level residual uncertainty in the recovered profiles.

All of these depth profiling techniques are of limited applicability in organic thin film systems for the reasons enumerated previously and because they are restricted to being performed in a high vacuum environment. This latter restriction is always a source of concern when the behavior of the thin film system in pertinent chemical environments is sought since its behavior may be different from when it is in vacuum. Furthermore, with the exception of chemical shift information from the photoelectron spectroscopic technique, only atomic information is available from these approaches.

III. DEPTH PROFILING WITH PHOTONS

The use of lower energy photons (e.g., UV-IR) in place of high energy particles, such as X-rays, ion, and high energy electrons, allows sampling in environments other than vacuum. This approach can also yield molecular information because molecular spectroscopic detection schemes can be coupled with the depth profiling protocol, whereas the higher energy vacuum techniques are more appropriate for obtaining information at the atomic level. Methods using these lower energy photons are discussed in the next sections.

A. Photoacoustic Spectroscopy

Photoacoustic spectroscopy (PAS) has been used successfully for depth-resolved determinations of molecular components in thin film systems in the UV-visible[67-69] and IR[70-78] spectral regions. In PAS experiments, use is made of the relationship between the modulation frequency and the thermal diffusion length. Depth profiling is achieved by varying the modulation frequency, which in turn varies the depth of sampling, typically between 10 and 60 μm for organic polymer systems in the IR and, between 1 to 10 μm in the UV-visible spectral regions. Since the sampling depth is dependent upon the modulation frequency, thermal diffusivity, and refractive in-

dex, for depth profiling applications, the sample must be both thermally thick and optically opaque (i.e., thermal diffusion length < optical pathlength < sample thickness).[75-78] Although many samples will satisfy this set of criteria, many others will not. In addition, highly desirable sample characteristics include a layered sample with components possessing very different spectral features, and structure which is either symmetrical or supported on a nontransparent substrate of high heat capacity.[74] Having sample components which have different electronic spectral signatures is a very low probability circumstance for organic polymers since many of the common functional groups found in polymers have electronic spectra which overlap. In the IR, this problem is relaxed somewhat due to the existence of group-specific absorption bands. Nevertheless, these requirements are somewhat restrictive, as is the small variability of the range of depth profiling and the large distances (in an absolute sense) over which the IR experiment works.

Moreover, some discretion must be used in the interpretation of the results since the variation of modulation frequency can lead to substantial sample cell resonance interferences and saturation effects, which can cause peak asymmetry or inversion.[72,74,75] These anomalies are most severe for depth profiling in the IR region, because the FT-IR modulation frequency varies considerably over the spectral region of 400 to 4000 cm^{-1}. Hence, in a single spectrum, the sampling depth varies by a factor of three.[74] This effect is convoluted with the dependence of the sampling depth on the refractive index. These difficulties have prohibited quantitative depth profiling unless the functional form of the dopant distribution is known and the sample is well characterized with respect to its optical transmission and thermal diffusivity. Frequently, internal standard techniques are employed to partially offset these difficulties, allowing semiquantitative conclusions to be derived.[69,75,78] However, saturation effects must still be cautiously considered.

B. Attenuated Total Reflection

Attenuated total reflection (ATR) spectroscopy has frequently been utilized for depth resolved analyses in the UV through the IR spectroscopic regions.[79-88] In the total internal reflection phenomenon, an evanescent field component extends a small distance into the low refractive index medium (containing the sample), as determined by Equation 1

$$d_p = \frac{\lambda}{2\pi\left(\sin^2\theta - \left(\frac{n_2}{n_1}\right)^2\right)^{1/2}} \qquad (1)$$

where d_p is the depth of penetration, λ is the wavelength of the incident radiation, n_2 and n_1 are the refractive indices of the rare and dense media, respectively, and θ is the angle of incidence in the dense medium. The evanescent field is also shown in Figure 2. Clearly, by changing the angle of incidence, the depth of penetration of the radiation into the external medium may be varied. Molecular transition dipoles in the external medium may interact with the evanescent field in the normal manner, giving rise to the attenuation in the total internal reflection signal. Then, the sample depth profile is recovered by inverting a set of integral equations corresponding formally

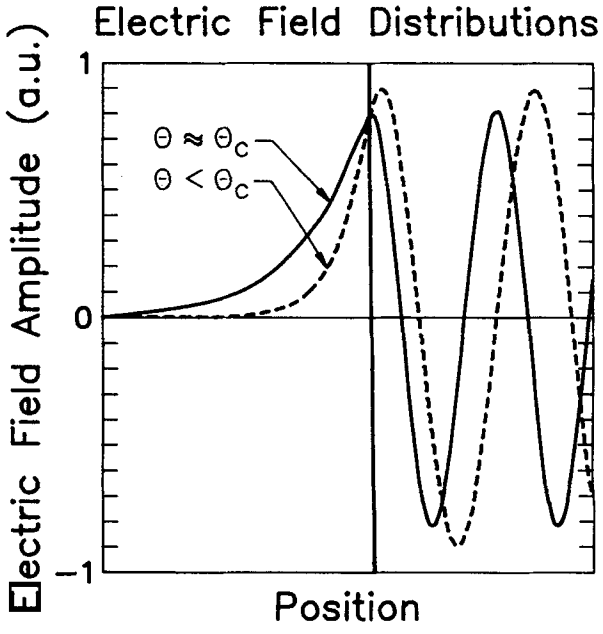

FIGURE 2. Plot of the interior and evanescent field amplitudes for total internal reflection implemented at two angles, one near the critical angle and one larger than the critical angle.

to Laplace transforms. As an example, FT-IR ATR has been used to determine film thickness in composite polymer systems.[80,81,85] The depth of penetration is dependent upon the excitation wavelength, excitation angle, and the refractive indices of the sample and substrate.[79,82,89] Typical sampling depths are approximately 0.1 μm in the UV-visible spectral region, increasing to 10 μm in the mid-IR.[79,82,90] A major strength of the technique is the ability to perform *in situ* experiments in realistic, even harsh, environments. Because radiation is guided in the internal reflection crystal, the optical properties of the absorbing system are unimportant as long as the refractive index remains below that of the guiding crystal. Usually IR or UV-visible transparent materials with very large refractive indices are readily available, so this requirement is not terribly stringent. A major restriction, however, is the inability to vary the sampling depth substantially for a single sample at a given excitation wavelength without a sophisticated mechanical design to vary the angle of excitation. In practice, this limits depth profiling studies to multiple samples, e.g., varying the substrate or undercoating thickness to alter the depth of excitation, or monitoring a time-dependent alteration. Both of these approaches lead to uncertainties in the actual sampling of the electric field intensity distribution due to sample-to-sample variations in refractive index, absorption coefficient, and scattering loss. These difficulties have prevented quantitative depth profiling experiments, except where multiple samples of varying thickness can be made and the functional form of the distribution is known beforehand.

Conventional PAS and ATR techniques allow only qualitative depth profiling information to be obtained unless the functional form of the dopant distribution is known (e.g., composites with step function distributions). In contrast, variable angle total internal reflection fluorescence (VA-TIRF) offers quantitative information without *a priori* information about the functional form of the dopant distribution.[91] In this experiment, the fluorescence from an adlayer on a solid substrate is used as signal, rather than the absorption of guided radiation. Of course, in the adlayer, absorption must precede fluorescent emission, so the same basic photophysical principles apply as in the conventional ATR experiment. The major operational difference resides in the method of extracting the signal. The VA-TIRF technique is still undergoing development, but its potential for measuring distributions with unknown functional forms is very promising. The technique is obviously limited to fluorescent molecules and molecules for which strong resonance Raman signals can be obtained, and the maximum profiling depth is approximately 1 to 5 μm.

Quantitative depth profiling experiments in the IR spectral region without functional form assumptions have been performed by Stuchebryukoa and co-workers[92] using another variation of the ATR technique. They report results from a solution-deposited 3.4-μm thick polymer film (terpolymer of ethylene, propylene, and dicyclopentadiene) which showed a 60% decrease in the absorption due to rocking vibrations of the CH_2 groups at the center of the film. The technique used combinations of leaky waveguide modes and frustrated internal reflection to obtain a set of spatially varying excitations in the profiled polymer film, which is deposited on an ATR crystal. A set of Fredholm integral equations result, describing the relationship between sample composition profile and signal. Solving these integral equations is difficult due to the extreme susceptibility of the results to small errors in the data *(vide infra)*. The extent, however, of ill-conditioning of the equations may be relaxed by including information from leaky modes in addition to conventional ATR sampling. Although the experiments were incompletely documented, the general approach taken is very closely related to the optical waveguide depth profiling experiment discussed extensively next.

C. Spectroscopic Ellipsometry

Ellipsometry is an experiment which measures the response of a surface to polarized radiation. The complex reflectivity of a sample is given by Equations 2 and 3,

$$\rho \equiv \frac{r_p}{r_s} = \tan \psi e^{i\Delta} \qquad (2)$$

$$\tan \psi = \frac{|r_p|}{|r_s|}; \Delta = \delta_p - \delta_s \qquad (3)$$

where $r_{s,p}$ are the complex amplitude reflectivities for s and p polarized optical radiation, respectively, and $\delta_{s,p}$ are phase shifts for s and p polarized radiation. Because the response depends on the optical properties of the sample, measurement of the ellipsometric parameters Δ and Ψ at a single wavelength and several angles of incidence is sufficient to define the optical properties (i.e., complex refractive index and physical thickness) of a thin surface film by inverting the reflectivity equations.[93] Naturally, if the film is absorbing, then only the response up to an absorption length in the film is obtained. Spectroscopic ellipsometry (SE) differs from single wavelength measurements in that measurements of the ellipsometric parameters are made at a large number of wavelengths throughout a given spectral region (typically, either 1.5 to 4.0 eV photon energy or the entire mid-IR.) Thus, information about the optical response throughout the spectral region is available, and because the thickness clearly does not change with wavelength of excitation, the optical parameters can be overdetermined. Once the optical parameters are known, they can be used to relate the composition as a function of depth through extensive use of modeling and the effective medium approximation. In the effective medium approach, the optical properties of a medium are assigned to a weighted average of several different compositional components of varying atomic polarizability. Effective medium methods can be successfully employed in pure dielectric media and in absorbing films. An example from a typical recovery is shown in Figure 3.

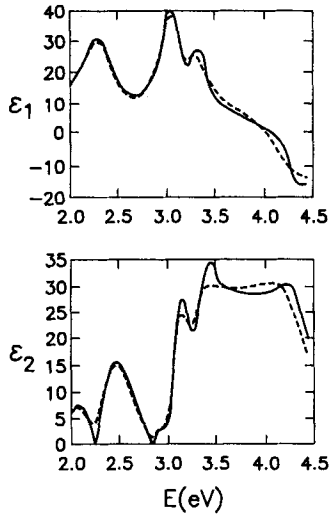

A

XTEM		SE	
SiO_2	25 Å	SiO_2	24 ± 3 Å
c-Si+a-si	120 ± 20 Å	$c\text{-}Si_{0.82}$ + $a\text{-}Si_{0.18 \pm 0.03}$	119 ± 19 Å
c-Si	550 ± 50 Å	$c\text{-}Si_{1.03 \pm 0.03}$	511 ± 21 Å
c-Si	250 ± 50 Å	$c\text{-}Si_{0.21}$ + $a\text{-}Si_{0.79 \pm 0.03}$	270 ± 30 Å
c-Si		c-Si	

B

FIGURE 3. (A) Plot of the calculated (- - - -) and measured (— — — —) spectral response for the real, ϵ_1, and imaginary, ϵ_2, parts of the dielectric function for the structure whose composition is profiled. (B) Depth profile recovered from spectroscopic ellipsometry (SE) and from X-ray transmission electron microscopy (XTEM) measurements. Note the excellent agreement between the two sets of measurements. (Adapted from Reference 95.)

SE has also been used for depth profiling in a variety of thin film materials.[94-97] The spectral range can be anywhere from the UV through the near-IR region, and it is typically used for films less than approximately 200-nm thick. Unfortunately, exact sample requirements for depth profiling have not been well defined in the literature. A common denominator in samples which have been successfully profiled with SE, however, include a highly absorbing substrate, and a film with a modest absorption band in the frequency range investigated. Frequently, *a priori* information about the functional form of the dopant distribution, obtained from other techniques, is utilized in modeling the optical response. Another approach, with a resolution of one tenth the total film thickness, has been illustrated by using a ten-layer model.[93] The major advantages of SE over other methods include nondestructive sampling, excellent detectivity (the detection limit by SE can be as small as 0.01 of a monolayer in optimum cases[36]), and applicability to ambient environments. The extreme sensitivity to surface

films, however, indicates that the technique is also very susceptible to surface contamination problems. Other difficulties include component defects and misalignment problems which contribute significant measurement errors. These errors prohibit the extension of the n-th layer model beyond approximately ten layers.[93] It should also be noted that it is the complex refractive index which is actually being depth profiled. Therefore, the relationship between analyte concentration and refractive index must always be known in order for quantitative results to be obtained.

D. Miscellaneous Photon-Based Techniques

Another interesting depth profiling technique involves FT-IR photothermal beam deflection spectroscopy. Experiments using bilayer samples consisting of a 20-μm nitrocellulose film supported on 20-, 30-, and 45-μm polyethylene sheets[98] have demonstrated the fundamentals of the method. The technique is very similar to PAS in many respects but circumvents resonant cell interferences since photodeflection is not affected by the sample cell structure. Unfortunately, the signal-to-noise (S/N) ratio decreases with increasing modulation frequencies, which, in practice, negates the advantages over PAS. An order of magnitude improvement in detection capabilities will be required to achieve a practical advantage over PAS. The technique is complementary to PAS since it is more suitable for samples with smooth surfaces, whereas optimal S/N is obtained from rough or porous samples in PAS.

Depth profiling in thin films can also be accomplished in some systems by determining the refractive index as a function of depth and assuming a relation between the index of refraction and the concentration of the dopant. This is effectively isomorphous with the effective medium approaches mentioned above. Many techniques can measure angle-dependent reflection or transmittance and fit the data to an assumed refractive index vs. depth functional form.[99,100] Unfortunately, the results are only as accurate as the functional form assumptions, and the inversion procedure required is ill-posed, leading to large sensitivity to small errors in the data.

E. Miscellaneous Techniques for Diffusion Studies

Several techniques have been developed for the sole purpose of obtaining information on diffusion in solid polymer films.[101,102] Temporally resolved spatial profiling experiments provide a direct means for studying diffusion processes. Studies of large polymer diffusion mechanisms, such as reptation, have generated substantial interest in techniques with the ability to measure very small diffusion coefficients.[103-108] One technique involves measuring the displacement of gold markers at a polymer interface via Rutherford backscattering spectroscopy.[109] The diffusion of the gold markers in different molecular weight polymers was used to measure the self-diffusion coefficient of the polymer. The technique suffers from possible sample perturbations due to the presence of the gold markers, and the necessity of correlating marker displacement and polymer diffusion via an appropriate model for the microscopic dynamics leading to diffusion.

A more recent method, which also uses high energy alpha particle bombardment, has been coined forward recoil spectroscopy (FRS).[110] In this technique, which was originally developed for profiling ^{1}H and ^{2}H in metals, a beam of $^{4}He^{2+}$ (E_0 = 3 MeV) strikes the sample at a shallow angle (typically 10 to 15°). Nuclei in the near surface region, including the ^{1}H and ^{2}H of interest, recoil from the surface due to elastic collisions with the incoming $^{4}He^{2+}$. Many ions are also scattered in the forward direction at an angle near 30°, but these are made to pass through a mylar stopping foil, whose primary purpose is to prevent heavier nuclei from reaching the detector. The atomic species of interest lose some energy upon traversing the mylar foil and are then incident on a particle energy sensitive detector. The number of particles at each pass energy is recorded on a multichannel analyzer. It is observed that ^{2}H nuclei recoiling from the surface do so with a much larger fraction of the initial energy of the incident $^{4}He^{2+}$ nuclei than do the ^{1}H nuclei. Thus, the two atomic species are well separated energetically. Nuclei which arise from a greater depth in the material will naturally have a higher probability of experiencing one or more inelastic collisions before emerging from the sur-

face region. Thus, each elastic surface peak is accompanied by a lower energy tail composed of nuclei originating from a greater depth in the sample. This distribution of nuclei at various inelastic energies lower than the elastic surface peak can be analyzed in a straightforward manner for the depth distribution of the pertinent nucleus. An example of a forward recoil spectrum for a bilayer film composed of deuterated and protonated polystyrene is shown in Figure 4.

This technique is capable of measuring depth profiles of deuterium and hydrogen in polymer films by measuring the energy distribution of the displaced ions. FRS experiments which monitor the diffusion of deuterated polymers into protonated polymers have been very successful,[110-116] although questions have recently arisen about the perturbations caused by deuterium labeling.[106,113,117] The maximum profiling range is approximately 1 μm,[110] and the typical resolution

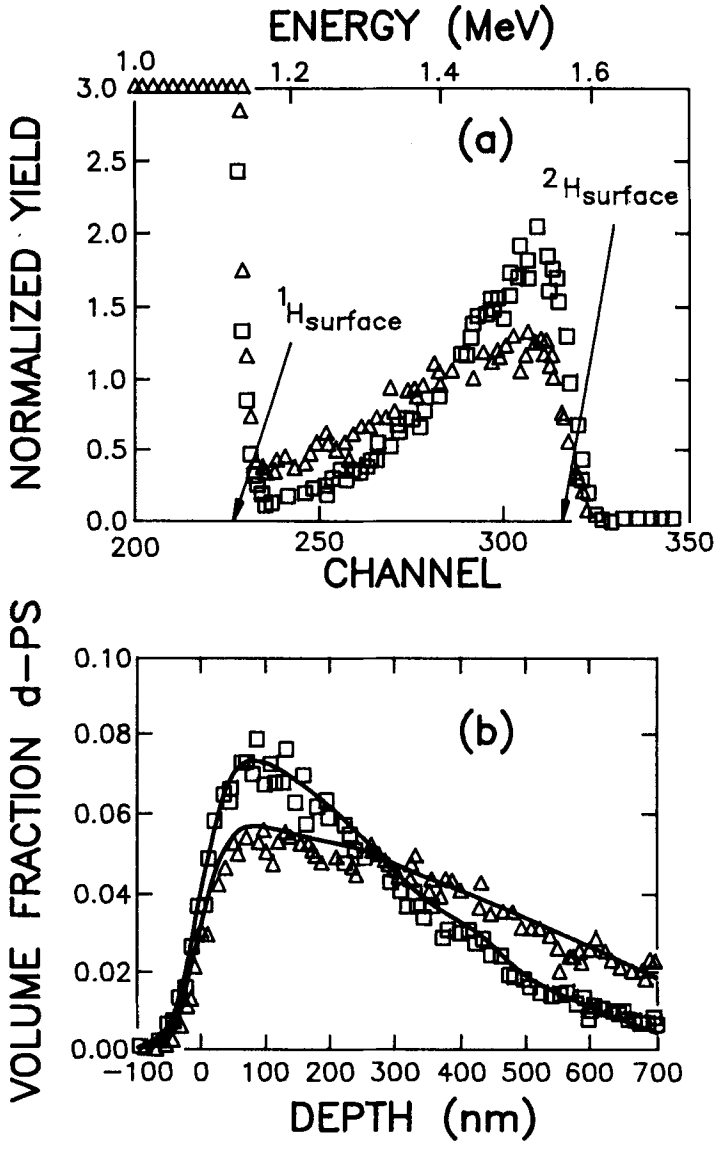

FIGURE 4. (a) Forward recoil spectra from poly(styrene-d_8)-poly(styrene) bilayers diffused at 170°C for 200 s. (b) Volume fraction of poly(styrene-d_8) as a function of depth, x. Poly(styrene) molecular weights are M = 36,000 (▲), M = 54,000 (■); poly(styrene-d_8) molecular weight is 110,000 in both cases. (Adapted from Reference 110.)

is 80 nm.[114] The range is limited by the necessity to avoid overlap between the low energy tail of the deuterium peak and the proton peak, while the resolution is typically limited due to straggling and detector limited energy resolution.[110,112] The technique is essentially nondestructive since the required sampling time is small compared to the rate of sample degradation, and typical sensitivity is approximately 0.1 atomic percent.[114] It also should be noted that functional form assumptions about the dopant distribution are not required. The dopant distribution is obtained directly because the sampling depth is related to the recoiled ion energy, and the concentration is proportional to the number of ions at that energy. The energy-to-depth relationship is determined from measurements on known samples or from stopping cross-section tables. The only major constraints involve the modest vacuum environment, the fact that only atomic information is obtained, and the limited sampling depth. Also, the required energy resolution will increase when more massive nuclei are measured. Still the application of this technique to other thin organic film systems and to processes other than diffusion should also be fruitful.

Another approach for measuring diffusion in polymer films utilizes small angle neutron scattering[118] or X-ray scattering[119] from alternating layered composites. This technique is less desirable than FRS due to sample fabrication requirements of multiple alternating layers with sharp boundaries and equal layer thicknesses; furthermore, functional form assumptions on the dopant distributions are required.

Fluorescence redistribution after pattern photobleaching also has been used to measure diffusion in a direction parallel to the film surface.[120] A physical mask is used with photobleaching illumination from a laser to create dopant depleted regions. Subsequently, the fluorescence intensity from nonbleached dopants diffusing into the depleted regions is probed. A variation of this technique involves using a holographic grating produced via interference between two coherent laser beams for pattern photobleaching. Diffusion of fluorescein-labeled polystyrene has been achieved with the grating approach.[121] A major advantage of the technique is that analyses can be performed under ambient conditions, and probably even in solution. Unfortunately, dopant distribution functional form assumptions must be made, and the technique is limited to monitoring the diffusion of fluorescent probes. This generally requires the dopant to be labeled in a manner which does not affect its diffusion properties, a requirement not easily satisfied and even harder to verify.

F. Planar Dielectric Optical Waveguides

Depth profiling experiments in planar optical waveguides share many of the limitations and successes of other photon-based techniques, and therefore, they are covered here in more detail. As shown in Figure 5, the electric field intensity in waveguides excited with different eigenmodes varies across the width of the guiding layer, leading naturally to the idea that spectroscopy carried out with these eigenmodes will carry information about the spatial distribution of the spectroscopically active species. Consider a hypothetical thin film, like the one shown in Figure 5, which supports three eigenmodes, and which has an exponentially decaying number density distribution of dopant. The signal should be proportional to the product of the electric field intensity and the number density at each point in space, then summed over all points. In the context of Figure 5, the value of such an integral would be proportional to the area under the product distributions on the right-hand side of the figure. In generic terms, we could write the intensity observed for excitation at the j-*th* eigenmode as

$$I_j = K_j \int_0^t E_j^2(z)N(z)\,dz \qquad (4)$$

where the symbols all have the same meaning as in the figure, and K_j is a mode-dependent constant, which depends on propagation losses, coupling efficiency, and proportionality constants. One value of I_j is obtained for each eigenmode excited, and the values of the electric field intensity distributions can be obtained with good accuracy from the measured coupling angles. Thus, depth profiling in planar waveguide structures distills down to finding an appropriate

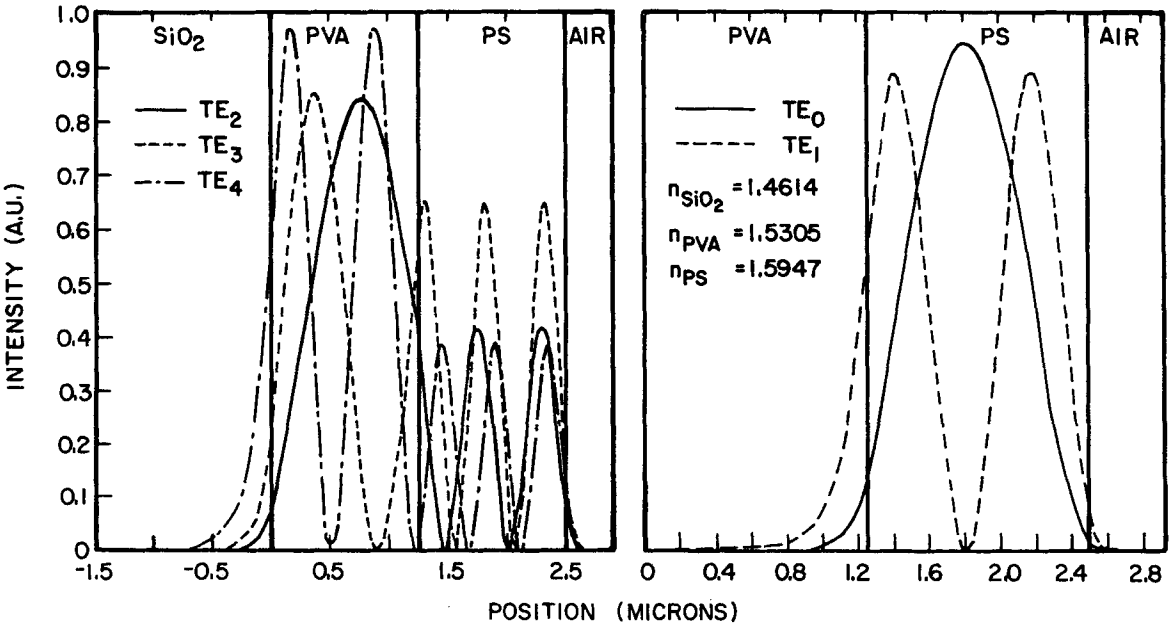

FIGURE 5. Plot of the electric field intensity as a function of spatial position in a polymer multilayer optical waveguide structure. This hypothetical structure consists of consecutive 1.25-μm thick layers of poly(vinyl alcohol) and poly(styrene) on fused silica. The TE_0 and TE_1 modes guide only in the poly(styrene) layer (right), while TE_2-TE_4 guide in both layers (left).

method of inverting the system of equations implied by Equation 4.

In fact, we can identify two separate types of problems to which waveguide-based optical depth profiling has been applied: those in which some *a priori* information about the functional form of the distribution exists (case 1), and those in which it does not (case 2). Case 1 can be characterized by assuming that the number density distribution is given by

$$N(z) = N(z; \alpha_1,\alpha_2,\ldots\alpha_n) \qquad (5)$$

where the α_i are parameters which specify the exact form of the distribution whose general form is known. Typically, knowledge of the functional form of the distribution implies some mechanistic information about how the dopant was introduced into the film.

For case 1 films, there are two challenges. First, the electric field intensity distributions in typical three-layer waveguides are nearly symmetric with respect to the center of the active guiding layer; the small asymmetry that is present arises from the mismatch in index discontinuities at the film-substrate and film-superstrate interfaces. The second problem stems from the fact that the signal equations (specific instances of Equation 4) are Fredholm integral equations of the first kind, a classic example of a mathematically ill-posed problem. Experimentally, this means that small errors in the measured spectroscopic intensities, I_j, will tend to introduce large errors into the recovered distributions, N(z). In addition, the number of eigenmodes supported by the film must equal or exceed the number of parameters to be recovered. Typically, the number of eigenmodes can always be increased by fabricating the layer of interest as an overlayer on top of a spectroscopically inert waveguide layer, which also solves the electric field symmetry problem.

One approach to dealing with case 1 samples involves direct examination of a hyperdimensional error surface, which is generated as follows. Characteristic peaks from the Raman or fluorescence spectrum of the dopant are measured for each of the eigenmodes excited in the structure to generate the experimental data vector, $\{I_j\}$. Then, a suitable region of the parameter

space to search is defined by $\alpha_{1,min}$, $\alpha_{1,max}$, $\alpha_{2,min}$, $\alpha_{2,max}$, . . . $\alpha_{n,min}$, $\alpha_{n,max}$, and an error function, $G(\alpha_i)$, defined by

$$G(\alpha_i) = \sum_{j=0}^{m} \left| I^2_{obs} - I^2_{calc}(\alpha_i) \right|^{1/2} \quad (6)$$

is then evaluated for all possible values of the parameters α_i within the selected range. The entire parameter space must be mapped because secondary minima in the error function exist, and location of the global minimum may be aided by the use of ancillary information *(vide infra)*. Of course, the set of α_i associated with the global minimum in $G(\alpha_i)$ is used to reconstruct the number density distribution in the sample.

Although information about the functional form of the distribution may be available in a significant number of problems, in many others it will not be. In inverting Equation 4 for case 2 problems, the recovery is severely underdetermined. A continuous distribution is to be recovered based on information from a finite number of measurements. The approach to this problem is adapted from the work of Phillips on general computational solutions to Fredholm integral equations.[122] Experimental error must be taken into account, so we rewrite Equation 4,

$$I_j + \epsilon_j = K_j \int_0^t E_j^2(z)N(z)\, dz \quad (7)$$

where ϵ_j describes the error for the j-*th* eigenmode. The problem of recovering the molecular distribution is not only ill-posed, it is also severely underdetermined, i.e., there are many members in the set of all possible solutions, $n = \{N_1, N_2, \ldots, N_f\}$. To find the correct solution, $N_s(z)$, a criterion is needed by which to distinguish it from the other members of the family of possible solutions. A maximum entropy criterion is formulated by which the correct distribution is the smoothest according to

$$\int_{\alpha_1}^{\alpha_2} (N_s'')^2\, dz = \min_{N\epsilon\nu} \int_{\alpha_1}^{\alpha_2} (N'')^2\, dz \quad (8)$$

To find N_s, one must first discretize the integrand,

$$I_j + \epsilon_j = \sum_{i=0}^{m} w_i K_j E_{ij} N_i \quad (9)$$

and require that the error be bounded,

$$\sum_{i=0}^{m} \epsilon_1^2 \leq e^2 \quad (10)$$

Then, the continuous minimization condition is replaced with a discrete one, i.e., seeking a function N_s which minimizes the sum of second differences,

$$\sum_{i=0}^{m} (N_{i+1,s} - 2N_{i,s} + N_{i-1,s})^2 = \min_{N\epsilon\nu} \sum_{i=0}^{m} (N_{i+1} - 2N_i + N_{i-1})^2 \quad (11)$$

The matrix element, A_{ij}, is introduced, as

$$A_{ij} \equiv w_i K_j E_{ij} \quad (12)$$

and the general element of its inverse,

$$A_{ij}^{-1} = \alpha_{ij} \quad (13)$$

and the matrix equation is then solved for N,

$$[N] = [A]^{-1}[I] + [A]^{-1}[\epsilon] \quad (14)$$

In order to obtain the smoothest solution according to the criterion defined above, one introduces a Lagrangian multiplier, γ, which has the effect of providing varying amounts of smoothing to the solutions. Thus,

$$\sum_{i=0}^{m} (N_{i+1,s} - 2N_{i,s} + N_{i-1,s}) (\alpha_{i+1,j} - 2\alpha_{ij} + \alpha_{i-1,j}) + \gamma^1\epsilon_j = 0; \quad j = 0,1,2,\ldots,m \quad (15)$$

In the actual experimental recoveries, γ is assumed to be known, and it is used to calculate the error vector, which is then compared to the experimental error bound, e^2. Model calculations are used to determine appropriate values for γ in

given situations, and the spread in the error vector allows one to perform model checks (e.g., randomness of the error vs. mode number).

First let us consider case 1 recoveries. Since the constants K_j change significantly over the range of modes encountered in a typical film, an internal standard approach was developed in which scattering from some homogeneously distributed component of the structure is used to ratio signal intensities from the various modes. Studies with model systems showed excellent agreement between calculated and observed intensity ratios when the internal standard technique was used. The simplest possible structures for which the functional form of the distribution could be known *a priori* are a Heaviside step function and a π-function distribution. In order to study these distributions, structures were fabricated with either two or three thin films, consisting of either protonated (PS) or deuterated (DPS) poly(styrene) and either protonated and deuterated poly(vinylpyridine) (P4VP). The unique feature of these structures is that the substitution of a nitrogen atom for a carbon atom at the 4-position of the aromatic side-group did not change the electronic polarizability significantly ($\Delta n = 0.001$, typically), but the vibrational dynamics of the aromatic ring were changed sufficiently to yield well-isolated bands in the Raman spectrum which were characteristic of the two. Thus, these samples are excellent examples of a situation in which molecular information can be extracted by exploiting group-specific vibrational information. The average discrepancy for all of the interfacial position determinations was 2.4%. It should also be pointed out that this error is far below the optical diffraction limit for these conditions. Thus, the accuracy of the recovery is limited not by physical effects, but rather by the precision with which the measurements can be made.

Next, structures for which the functional form of the distribution was not known *a priori* were examined. For these structures, a new method of handling the asymmetry problem was developed, which made the electric field intensity distributions asymmetric and allowed the recoveries to be obtained with single eigenmodes. Since only six modes were available for recovery in this sample, the recovery using only single modes and covering the entire film was both inaccurate and had low resolution. Therefore, the film to be profiled was placed as an overlayer on a spectroscopically inert waveguiding layer. When only the outer region of a two film structure was profiled, dramatic improvement in the resolution and accuracy of the compositional recovery were obtained. Recoveries were performed for values of the Lagrangian multiplier covering many orders of magnitude, and two striking features were noted. First, the recovery at the optimum γ value was excellent. Second, changing the value of γ over an order of magnitude still gave a respectable estimate of the molecular distribution. Thus, the recovery procedure employing the Lagrangian multiplier is computationally robust. At this point, it should also be noted that, contrary to intuition, the smoother the profile, the more difficult it is to recover in case 2 samples. This is essentially a precision problem. The more the sample distribution changes through a particular region, the more variation there is between different eigenmodes, and the better the recovery. This recovery algorithm was tested by examining the interdiffusion of poly(styrene-d_8) (DPS) into poly(styrene). A sample of DPS was coated onto a substrate, and then a PS film was floated off a water surface onto the DPS. This procedure was necessary in order to avoid dissolving the DPS in the solvent used to put down the PS. After fabrication and drying, the entire structure was heated above its glass transition temperature. The initial sharp boundary between the two materials was replaced by a gradual diffusion profile. Recovery of the new DPS profile was accomplished by monitoring C-D Raman scattering in the DPS vs. eigenmode, and excellent results were obtained.[123-126]

There are several limitations to the waveguide-based ODP experiment. First, there is clearly a point beyond which the spatial resolution cannot be pushed. As stated above, this is more an issue of precision than a fundamental physical limit. It is reasonable to expect that, at best, 200 to 400 Å resolution might be attained. This could be accomplished, for example, with a 2000 Å overlayer on a 5-μm waveguide of refractive index 1.6. The second limitation derives from the optical properties of the materials to be studied. In order for these quantitative ex-

periments to work, optical transparency along with a very good thickness and index uniformity are required. Finally, the materials limitation, up to this point, has prevented the use of metallic components in waveguide structures because metals are lossy typically limit the propagation length to <1 mm. However, the waveguide-based depth profiling experiment does not require long propagation lengths, and it is reasonable to expect that experiments could be carried out on metal-containing structures (e.g., electrodes covered with thin films of organic materials) *in situ*.

In summary, waveguide-based optical depth profiling experiments have been successfully applied to films in which the refractive index is homogeneous, meaning that the dopant concentrations in the guiding layer do not significantly alter the refractive index as a function of depth. Advantages of the technique include nondestructive sampling (with the exception of potential photobleaching, which can be circumvented through the use of near-IR Raman scattering), sub-diffraction limited resolution, no functional form assumptions, the attainment of molecular instead of simply atomic information, and a variety of allowable experimental environments (i.e., air, vacuum, and solution). The disadvantages are the significant sample restrictions caused by the need to configure the sample as an asymmetric slab dielectric optical waveguide. This and other prerequisites effectively limit the film's thickness to approximately 1 to 4 μm for organic films and to refractive indices above 1.49 (or 1.39 for MgF_2 substrates). The experiment is also technically challenging.

G. Refractive Index Profiling in Planar Waveguides

Waveguide-based experiments for optical depth profiling have also been successfully performed in films in which the refractive index is spatially inhomogeneous. These techniques are applicable when a dopant is sufficiently concentrated to alter substantially the refractive index of the waveguide. The dopant distribution is obtained indirectly since the refractive index is actually being profiled. Therefore, the relationship between the index of refraction and dopant concentration must be known, e.g., using the effective medium approaches mentioned in the section on spectroscopic ellipsometry *(vide supra)*. Early approaches involved using the measured resonant waveguiding angles. The discrepancy between the measured angles and the calculated resonant angles (or the calculated effective indices) for the parameters of an assumed functional form are minimized, resulting in the best fit depth profile.[57,127-129] This technique obviously requires explicit assumptions about the functional form of the refractive index profile. More recently, WKB methods have been developed which also utilize the measured perturbations of the waveguiding resonant angles, but do not require refractive index functional form assumptions.[130-133] The resolution of the technique is determined by the number of modes supported by the waveguide structure since the depth profile step size is simply the film thickness divided by the number of modes. A completely different approach, which is also free of functional form assumptions, uses direct measurements of the electric field intensity profile for the zeroth order mode. The refractive index distribution is calculated from the measured intensity profile.[134] Ti diffused $LiNbO_3$ strip waveguides have been profiled in both lateral and depth dimensions with a diffraction limited resolution of approximately 1 μm with this technique.

In addition, a series of recent studies in the author's laboratory have used the recovery of a two-component, time-dependent refractive index profile to characterize case II diffusion.[135] When thin polymer films are subjected to certain solvents, the uptake of solvent into the film is governed, not by the classical Fickian diffusion behavior, but rather by an anomalous behavior, which is termed case II diffusion. One of the characteristic features of the case II behavior is a very sharp solvent front which propagates linearly in time through the film. In order to characterize this behavior for a poly(styrene)/n-hexane system, the eigenmode distribution of a grating-coupled waveguide was followed as a function of time after immersion of the film in the solvent. The eigenmodes were then fit to a model in which the film was divided into two regions; one which was solvent swollen and had the refractive index of the final completely swollen film at equilib-

rium, and another nonswollen region which had the refractive index of the dry film. The former region grew linearly in time at the expense of the latter region.

IV. CONCLUSIONS

Depth resolved determinations of composition are frequently difficult or impossible to perform in a quantitative manner for nonconducting thin organic polymer films. Yet, this class of thin films is of huge importance in research and technology. One would like a technique to yield information which is (1) obtained in an *in situ* manner, (2) quantitative, (3) molecular, (4) obtained without *a priori* assumptions about the functional form of the distribution, and, of course, (5) highly resolved in the depth and lateral dimensions. None of the techniques developed to-date meet all of these ideal criteria. The most notable difficulty for these techniques are the sample limitations, which frequently include limited film thickness ranges, refractive index or thermal conductivity restrictions, and the necessity to make assumptions about the functional form of the dopant profile. Thus, the choice of a particular approach to obtaining depth profile information in an organic film system will necessarily involve a number of tradeoffs and careful consideration of the particular strengths and weaknesses of each technique. Of the techniques reviewed for depth profiling in organic thin films, FRS appears to be the most promising method for depth profiling of atomic compositional information. Dopant selectivity is easily achieved by deuteration, and dopant functional form assumptions are not needed. The major problems for FRS, however, are the required moderate vacuum environment and the lack of molecular information. The most promising technique for obtaining depth profiles with molecular information involves the use of optical waveguides. The sample requirements, although complementary to the other techniques, will limit the general utility of optical waveguide-based depth profiling. Finally, if the sample can be profitably profiled by recovery of the refractive index vs. depth, then SE is very powerful. However, it is necessary to have a good understanding of the relationship between composition and refractive index, an understanding which is probably only available in a few widely studied systems.

ACKNOWLEDGMENT

Work described herein which was performed in the author's laboratory was supported by the Department of Energy and by the donors of the Petroleum Research Fund of the American Chemical Society.

REFERENCES

1. **Schroeder, H.,** *Phys. Thin Films,* 5, 87, 1969.
2. **Sakka, S. and Kamiya, K.,** *J. Non-Cryst. Solids,* 42, 403, 1980.
3. **Yoldas, B. E.,** *Appl. Opt.,* 19, 1425, 1980.
4. **Klein, L. C. and Garvey, G. J.,** *Soluble Silicates,* Falcone, J. S., Jr., Ed., American Chemical Society, Washington, D.C., 1982, chap. 18.
5. **Mukherjee, S. P. and Lowdermilk, W. H.,** *Appl. Opt.,* 21, 293, 1982.
6. **Yoldas, B. E.,** *Appl. Opt.,* 21, 2960, 1982.
7. **Arfston, N. J., Kaufmann, R., and Dislich, H.,** *Ultrastructure Processing of Ceramics, Glasses and Composites,* Hench, L. L. and Ulrich, D. R., Eds., John Wiley & Sons, New York, 1984, chap. 15.
8. **Pulker, H. K.,** *Coatings on Glass,* Elsevier, New York, 1984.
9. **Cachard, A.,** *Glass . . . Current Issues,* Wright, A. F. and Dupuy, J., Eds., Martinus Nijhoff, Boston, 1985, 336.
10. **Rand, M. J. and Standley, R. D.,** *Appl. Opt.,* 11, 2482, 1972.
11. **Sosnowski, T. P. and Weber, H. P.,** *Appl. Phys. Lett.,* 21, 310, 1972.
12. **Tien, P. K., Smolinsky, F., and Martin, R. J.,** *Appl. Opt.,* 11, 637, 1972.
13. **Ulrich, R. and Weber, H. P.,** *Appl. Opt.,* 11, 428, 1972.
14. **Ramaswany, V. and Weber, H. P.,** *Appl. Opt.,* 12, 1581, 1973.
15. **Zernike, F.,** *Integrated Optics,* Vol. 7, Tamir, T., Ed., Springer-Verlag, New York, 1975, chap. 5.
16. **Tiefenthaler, K., Briguet, V., Buser, E., Horisberger, M., and Lukosz, W.,** *Thin Film Tech.,* 401, 165, 1983.
17. **Henry, C. H., Kazarinov, R. F., Lee, H. J., Orlowsky, K. J., and Katz, L. E.,** *Appl. Opt.,* 26, 2621, 1987.
18. **Kesting, R. E.,** *Synthetic Polymeric Membranes,* John Wiley & Sons, New York, 1985.
19. **Petropoulous, J. H.,** *Advances in Polymer Science,* Vol. 84, Springer-Verlag, New York, 1985, 93.

20. **Oyama, N., Yamaguchi, S., Kaneko, M., and Yamada, A.,** *J. Electroanal. Chem.*, 139, 215, 1982.
21. **Oyama, N., Oki, N., Ohni, H., Ohnuki, Y., Matsuda, H., and Tsuchida, E.,** *J. Phys. Chem.*, 87, 3642, 1983.
22. **Faulkner, L. R.,** *Chem. Eng. News*, 28, Feb. 27, 1984.
23. **Hupp, J. T., Otruba, J. P., Parus, S. J., and Meyer, T. J.,** *J. Electroanal. Chem.*, 190, 287, 1985.
24. **Calcaterra, L. T., Closs, G. L., and Miller, J. R.,** *J. Am. Chem. Soc.*, 105, 670, 1983.
25. **Kaneko, M., Moriya, S., Yamada, A., Yamamoto, H., and Oyama, N.,** *Electrochim. Acta*, 29, 115, 1984.
26. **Kaneko, M. and Yamada, A.,** *Advances in Polymer Science*, Vol. 55, Springer-Verlag, New York, 1984.
27. **Hargreaves, J. S. and Webber, S. E.,** *Macromolecules*, 18, 734, 1985.
28. **Shoop, C.,** thesis, University of Illinois at Urbana-Champaign, 1985.
29. **Bolts, J. M., Bocarsly, A. B., Palazzoto, M. C., Walton, E. G., Lewis, N. S., and Wrighton, M. S.,** *J. Am. Chem. Soc.*, 101, 1378, 1979.
30. **Noufi, R., Tench, D., and Warren, L. R.,** *J. Electrochem. Soc.*, 127, 2310, 1980.
31. **Sumitomo, H. and Hashimoto, K.,** *Advances in Polymer Science*, Vol. 64, Springer-Verlag, New York, 1985, 63.
32. **Heavens, O. S.,** *Optical Properties of Thin Solid Films*, Dover Publications, New York, 1965, chap. 5.
33. **Maissel, L. I. and Glang, R.,** *Handbook of Thin Film Technology*, McGraw-Hill, St. Louis, 1970.
34. **Ulrich, R. and Torge, R.,** *Appl. Opt.*, 12, 2901, 1973.
35. **Walter, D. J.,** *Thin Solid Films*, 23, 153, 1974.
36. **Aspnes, D. E. and Studna, A. A.,** *Appl. Opt.*, 14, 220, 1975.
37. **Kersten, R. T.,** *Opt. Acta*, 22, 515, 1975.
38. **Kersten, R. T.,** *Opt. Acta*, 22, 503, 1975.
39. **Swalen, J. D., Tacke, M., Santo, R., and Fischer, J.,** *Opt. Commun.*, 18, 387, 1976.
40. **Demner, Y. and Shamir, J.,** *Appl. Opt.*, 17, 3738, 1978.
41. **Westwood, W. D. and Wei, J. S.,** *Can. J. Phys.*, 57, 1247, 1979.
42. **Herrman, P. P.,** *Appl. Opt.*, 19, 3261, 1980.
43. **King, R. J. and Talim, S. P.,** *Opt. Acta*, 28, 1107, 1981.
44. **Bosacchi, B. and Oehrle, R. C.,** *Appl. Opt.*, 21, 2167, 1982.
45. **Ding, T. and Garmire, E.,** *Appl. Opt.*, 22, 3177, 1983.
46. **Bovard, B., Van Milligen, F. J., Messerly, M. J., Saxe, S. G., and Macleod, H. A.,** *Appl. Opt.*, 24, 1803, 1985.
47. **Hodgkinson, I. J., Horowitz, F., Macleod, H. A., Sikkens, M., and Wharton, J. J.,** *J. Opt. Soc. Am. A*, 2, 1693, 1985.
48. **Palmer, K. F. and Williams, M. Z.,** *Appl. Opt.*, 24, 1788, 1985.
49. **Swanepoel, R.,** *J. Opt. Soc. Am. A*, 2, 1339, 1985.
50. **Hill, J. M., Royce, D. G., Fadley, C. S., Wagner, L. R., and Grunthaner, F. J.,** *Chem. Phys. Lett.*, 44, 225, 1976.
51. **Clark, D. T., Dilks, A., Shuttleworth, D., and Thomas, H. R.,** *J. Electron Spectrosc. Relat. Phenom.*, 14, 247, 1978.
52. **Umana, M., Denisevich, P., Rolison, D. R., Nakahama, S., and Murray, R. W.,** *Anal. Chem.*, 53, 1170, 1981.
53. **Mathieu, H. J. and Landolt, D.,** *Surf. Interface Anal.*, 6, 82, 1984.
54. **Powell, C. J.,** *Surf. Interface Anal.*, 7, 256, 1985.
55. **Dobrott, R. D.,** *Electrochem. Soc. Ext. Abstr.*, 100, 250, 1975.
56. **Tarng, M. L. and Fisher, D. G.,** *J. Vac. Sci. Technol.*, 15, 50, 1978.
57. **Griffiths, G. and Khan, P. J.,** *IEEE J. Quantum Electron*, QE-17, 529, 1981.
58. **Magee, C. W. and Honig, R. E.,** *Surf. Interface Anal.*, 4, 35, 1982.
59. **Hayes, M.,** *Surf. Technol.*, 20, 3, 1983.
60. **Gries, H. W.,** *Surf. Interface Anal.*, 7, 29, 1985.
61. **Narayan, J. and Holland, O. W.,** *Phys. Status Solidi*, 73, 242, 1982.
62. **Holland, O. W., Appleton, B. R., and Narayan, J.,** *J. Appl. Phys.*, 54, 2295, 1983.
63. **Magee, C. W. and Harrington, W. L.,** *Appl. Phys. Lett.*, 33, 193, 1978.
64. **Coburn, J. W.,** *J. Vac. Sci. Technol.*, 13, 1037, 1976.
65. **Wittmaack, K.,** *Surf. Sci.*, 89, 668, 1979.
66. **Surridge, N. A., Linton, R. W., Hupp, J. T., Bryan, S. R., Meyer, T. J., and Griffis, D. P.,** *Anal. Chem.*, 58, 2443, 1986.
67. **Rosenewaig, A. and Greshro, A.,** *J. Appl. Phys.*, 47, 64, 1976.
68. **Rosenewaig, A.,** *Opt. Commun.*, 7, 305, 1978.
69. **Rosenewaig, A.,** *Photoacoustics and Photoacoustic Spectroscopy*, John Wiley & Sons, New York, 1980.
70. **Carlsson, D. J. and Wiles, D. M.,** *Can. J. Chem.*, 48, 2397, 1970.
71. **Webb, J. B.,** *J. Polym. Sci.*, A-1(10), 2335, 1972.
72. **Krishnan, K.,** *Appl. Spectrosc.*, 35, 549, 1981.
73. **Gerson, D. J., Wong, J. S., and Casper, J. M.,** *Am. Lab.*, 16, 63, 1984.
74. **Donini, J. C. and Michaelian, K. H.,** *Infrared Phys.*, 24, 157, 1984.
75. **Urban, M. W. and Koenig, J. L.,** *Appl. Spectrosc.*, 40, 944, 1986.
76. **Yang, C. Q. and Fateley, W. G.,** *Polym. Mater. Sci. Eng.*, 54, 404, 1986.
77. **Yang, C. Q. and Fateley, W. G.,** *Anal. Chim. Acta*, 194, 303, 1987.
78. **Yang, C. Q., Bresee, R. R., and Fateley, W. G.,** *Appl. Spectrosc.*, 41, 889, 1987.

79. **Harrick, N. J.,** *Internal Reflection Spectroscopy,* Wiley-Interscience, New York, 1967.
80. **Tompkins, H. G.,** *Appl. Spectrosc.,* 28, 335, 1974.
81. **Blackwell, C. S., Degen, P. J., and Osterholz, F. D.,** *Appl. Spectrosc.,* 32, 480, 1978.
82. **Epstein, D. J.,** *Appl. Spectrosc.,* 34, 233, 1980.
83. **Allain, C., Ausserre, D., and Rondelez, F.,** *Phys. Rev. Lett.,* 49, 1694, 1982.
84. **Ohta, K. and Iwamoto, R.,** *Anal. Chem.,* 57, 2491, 1985.
85. **Ohta, K. and Iwamoto, R.,** *Appl. Spectrosc.,* 39, 418, 1985.
86. **Kellner, R., Kashofer, F., and Simeonov, V.,** *Fresenius Z. Anal, Chem.,* 325, 258, 1986.
87. **Luoma, G. A. and Rowland, R. D.,** *J. Appl. Polym. Sci.,* 32, 5777, 1986.
88. **Kuhn, K. J., Hahn, B., Percec, V., and Urban, M. W.,** *Appl. Spectrosc.,* 41, 843, 1987.
89. **Mahan, A. I. and Bitterli, C. V.,** *Appl. Opt.,* 17, 509, 1978.
90. **Saucy, D. A., Simko, S. J., and Linton, R. W.,** *Anal. Chem.,* 57, 871, 1985.
91. **Reichert, W. M., Sui, P. A., Ives, J. T., and Andrade, J. D.,** *Appl. Spectrosc.,* 41, 503, 1987.
92. **Stuchebryukov, S. D., Vavkushevsky, A. A., and Rudoy, V. M.,** *Surf. Interface Anal.,* 6, 29, 1984.
93. **Erman, E. and Theeten, J. B.,** *Surf. Interface Anal.,* 4, 98, 1982.
94. **Vedam, K., McMan, P. J., and Narayan, J.,** *Appl. Phys.,* 47, 229, 1985.
95. **McMan, P. J., Vedam, K., and Narayan, J.,** *J. Appl. Phys.,* 59, 694, 1986.
96. **McMarr, P. J., Blanco, J. R., Vedam, K., Messier, R., and Dilione, L.,** *Appl. Phys. Lett.,* 49, 328, 1986.
97. **Vedam, K., Kim, S. Y., Aries, L. D., and Guenther, A. H.,** *Opt. Lett.,* 12, 456, 1987.
98. **Varlashkin, P. G. and Low, M. J. D.,** *Infrared Phys.,* 26, 171, 1986.
99. **Grimbergen, M. N. and Goldner, R. B.,** Proceedings of SPIE — The International Society for Optical Engineering, *Thin Film Technol.,* 401, 198, 1983.
100. **Borgogno, J. P., Flory, F., Rouche, P., Schmitt, B., Albrand, G., Pelletier, E., and Macleod, H. A.,** *Appl. Opt.,* 23, 3567, 1984.
101. **von Meerwall, E. D.,** *Adv. Polym. Sci.,* 54, 1, 1984.
102. **Tirrell, M.,** *Rubber Chem. Technol.,* 57, 523, 1984.
103. **Klein, J.,** *Nature,* 271, 143, 1978.
104. **Klein, J. and Briscoe, B. J.,** *Proc. R. Soc. London A,* 365, 53, 1979.
105. **Smith, B. A., Samulski, E. T., Yu, L. P., and Winnik, M. A.,** *Phys. Rev. Lett.,* 52, 45, 1984.
106. **McKenna, G. B.,** *Polym. Commun.,* 26, 324, 1985.
107. **Klein, J.,** *Macromolecules,* 19, 105, 1986.
108. **Keith, H. D. and Padden, F. J., Jr.,** *J. Polym. Sci. B: Polym. Phys.,* 25, 229, 1987.
109. **Green, P. F., Palmstrom, C. J., Mayer, J. W., and Kramer, E. J.,** *Macromolecules,* 18, 501, 1985.
110. **Green, P. F., Mills, P. J., Palmstrom, C. J., Mayer, J. W., and Kramer, E. J.,** *Phys. Rev. Lett.,* 53, 2145, 1984.
111. **Composto, R. J., Mayer, J. W., Kramer, E. J., and White, D. M.,** *Phys. Rev. Lett.,* 57, 1312, 1986.
112. **Feldman, L. C. and Mayer, J. W.,** *Fundamentals of Surface and Thin Film Analysis,* Elsevier, New York, 1986.
113. **Green, P. F. and Doyle, B. L.,** *Phys. Rev. Lett.,* 57, 2407, 1986.
114. **Green, P. F., Mills, P. J., and Kramer, E. J.,** *Polymer,* 27, 1063, 1986.
115. **Mills, P. J., Green, P. F., Palmstrom, C. J., Mayer, J. W., and Kramer, E. J.,** *J. Polym. Sci. Polym. Phys. Ed.,* 24, 1, 1986.
116. **Mills, P. J., Mayer, J. W., Kramer, E. J., Hadziioannou, G., Lutz, P., Strazielle, C., Rempp, P., and Kovacs, A. J.,** *Macromolecules,* 20, 513, 1987.
117. **Yang, H., Stein, R. S., Han, C. C., Bauer, B. J., and Kramer, E. J.,** *Polym. Commun.,* 27, 132, 1986.
118. **Bartels, C. R., Graessley, W. W., and Crist, B.,** *J. Polym. Sci. Polym. Lett. Ed.,* 21, 495, 1983.
119. **Hashimoto, T., Tsukahara, Y., and Kawai, K.,** *Macromolecules,* 14, 708, 1981.
120. **Smith, B. A.,** *Macromolecules,* 15, 469, 1982.
121. **Antoniette, M., Coutandin, J., Grutter, R., and Sillescu, H.,** *Macromolecules,* 17, 798, 1984.
122. **Phillips, D. L.,** *J. Assoc. Comp. Mach.,* 9, 84, 1962.
123. **Miller, D. R., Han, O. H., and Bohn, P. W.,** *Appl. Spectrosc.,* 41, 245, 1987.
124. **Miller, D. R., Han, O. H., and Bohn, P. W.,** *Appl. Spectrosc.,* 41, 249, 1987.
125. **Miller, D. R. and Bohn, P. W.,** *Anal. Chem.,* 60, 407, 1988.
126. **Miller, D. R. and Bohn, P. W.,** *Appl. Opt.,* 27, 2566, 1988.
127. **Sarid, D.,** *Appl. Opt.,* 19, 1606, 1980.
128. **Albert, J. and Yip, G. L.,** *Appl. Opt.,* 24, 3692, 1985.
129. **Danko, J. J. and Ryan-Howard, D. P.,** *Appl. Opt.,* 25, 1505, 1986.
130. **Chiang, K. S.,** *J. Lightwave Technol.,* LT-3, 385, 1985.
131. **Arutunyan, E. A. and Galoyan, S. K.,** *Opt. Commun.,* 56, 399, 1986.
132. **Canali, C., DeBernardi, C., De Sanio M., Loffredo, A., Mazzi, G., and Morasca, J. S.,** *Lightwave Technol.,* LT-4, 951, 1986.
133. **Chandler, P. J. and Lama, F. L.,** *Opt. Acta,* 33, 127, 1986.
134. **Chandler, P. J. and Lama, F. L.,** *Opt. Acta,* 33, 127, 1986.
135. **Bohn, P. W. and Fell, N. F.,** *Proc. Soc. Photo-Opt. Eng.,* 909, 130, 1989.